Self-blinking dye restores efficient use of nanobodies in single-molecule localization microscopy.

Samrat Basak[1,2], Kaushik Inamdar[3,4], Yoav G. Pollack[5], László Albert[6,7], Daniel C. Jans[3,4], Stefan Jakobs[3,4,8,9], Jörg Enderlein[1,9], Roman Tsukanov[1,*] and Felipe Opazo[6,7,10,*]

1. III. Institute of Physics - Biophysics, Georg-August University, 37077 Göttingen, Germany.
2. Department of Chemistry and Center for NanoScience, Ludwig-Maximilians-Universität München, Butenandtstr. 5-13, 81377 München, Germany.
3. Department of NanoBiophotonics, Max Planck Institute for Multidisciplinary Sciences, 37077 Göttingen, Germany.
4. Department of Neurology, University Medical Center Göttingen, 37073 Göttingen, Germany.
5. Institute for the Dynamics of Complex Systems, Georg-August University, 37077 Göttingen, Germany.
6. Center for Biostructural Imaging of Neurodegeneration (BIN), University Medical Center Göttingen, 37075 Göttingen, Germany.
7. Institute of Neuro-and Sensory Physiology, University Medical Center Göttingen, 37073 Göttingen, Germany.
8. Translational Neuroinflammation and Automated Microscopy, Fraunhofer Institute for Translational Medicine and Pharmacology ITMP, 37073 Göttingen, Germany.
9. Cluster of Excellence "Multiscale Bioimaging: from Molecular Machines to Networks of Excitable Cells" (MBExC), Georg-August University, Göttingen, Germany.
10. NanoTag Biotechnologies GmbH, 37079 Göttingen, Germany.

Emails fopazo@gwdg.de; rtsukan@gwdg.de

Abstract

Direct STORM relies on robust fluorophore blinking; observations suggest that AlexaFluor647 underperforms when coupled to nanobodies, thereby undermining the advantages of nanobodies. We show that the self-blinking dye JF635b preserves excellent blinking behavior upon nanobody conjugation, enabling sparse, stable localizations in saline buffers. Using these self-blinking nanobodies, we obtained robust dSTORM, FL-SMLM, and MINFLUX images, achieving localization precision of ~1 nm. Its simple implementation improves reproducibility and makes single-molecule localization microscopy more accessible.

Main Text

Single-molecule localization microscopy (SMLM)[1] enables nanometer-scale localization precision. Among its core implementations, direct stochastic optical reconstruction microscopy (dSTORM)[2] routinely achieves localization precision below 20 nm, but performance critically depends on the fluorophore blinking characteristics. AlexaFluor647 (AF647) has long been the benchmark dye, exhibiting robust blinking in buffers such as GLOX-MEA[2]. The reductive properties of the blinking buffers alter disulfide bonds in antibodies and nanobodies, weakening them or rendering them dysfunctional. Therefore, careful optimization of buffer composition for each sample is required, especially in multitarget imaging, which often requires compromises, leading to the development of sequential-labeling strategies such as NanoPlex[3].

Linkage error in indirect immunofluorescence (IF) labeling occurs when the primary antibody (1.Ab) targeting the protein of interest (POI) is labeled with a fluorescent secondary antibody (2.Ab). Indirect IF displaces fluorophores by up to 25 nm from the POI. Nanobodies (Nbs) reduce this to approximately 3 nm, making them ideal probes[4] for SMLM nanoscopy. However, AF647 underperforms when directly conjugated to most Nbs, exhibiting reduced blinking and photostability, thereby degrading image quality in blinking-dependent techniques.

Self-blinking dyes provide an elegant solution by spontaneously cycling between bright and dark states without the need for blinking-reducing buffers. Several such fluorophores have been explored for super-resolution microscopy, including specialized dyes for live-cell super-resolution imaging[5], Thioflavin T for fibrils[6], rhodamine-coumarin hybrids[7], silicon rhodamine analogues for STORM-MINFLUX[8], and rhodamine-based dyes for SOFI[9].

JF635b is a newly developed, spontaneously blinking rhodamine from the hydroxymethyl-SiR Janelia Fluor series, described in Holland et al.[10]. It exhibits an excellent duty cycle, is ideally suited to SMLM applications, and operates without reducing-blinking buffers, significantly simplifying the imaging workflow and making it compatible with a wide range of labeling strategies. Although its photophysical properties have been characterized when conjugated to HaloTags[10], its potential to address a key limitation in the blinking behavior of AF647 on Nbs has not been explored. Here, we benchmark JF635b against AF647 across Ab and Nb conjugates using wide-field self-blinking dSTORM (sb-dSTORM), confocal FL-SMLM[11,12], and MINFLUX[13].

We first compared dSTORM imaging of COS-7 cells transfected with TOMM70-EGFP-ALFA-tag, immunostained with two broadly used Nbs, binding EGFP (NbGFP) or ALFA-tag (NbALFA) conjugated to AF647 or JF635b. Imaging conditions were identical, except AF647 samples were imaged under GLOX-MEA buffer, while JF635b samples were imaged in PBS (Fig. 1; Supp. Fig.1 & Supp Table 1).

AF647 conjugated Nbs showed reduced blinking performance, fewer photons, shorter on-times, and most molecules bleached within ~10,000 frames compared to a control condition where the ALFA-tag was stained using conventional indirect IF, resulting in ~70% lower localization density, consistent for both NbGFP and NbALFA. Despite similar affinities, NbGFP-AF647 outperformed NbALFA-AF647 in reconstructing mitochondria tagged with EGFP and ALFA-tag accordingly. Specifically, NbALFA-AF647 showed poor blinking and rapid photobleaching, resulting in clearly suboptimal images. Because NbALFA withstands reducing conditions[14], the deficiencies are likely due to AF647's compromised blinking performance on Nbs. However, when using these Nbs conjugated to JF635b, bright emission bursts of ~500-1500 photons, on-times of 40-60ms, and sustained blinking over tens of thousands of frames without significant bleaching were observed in PBS buffer (Supp Movies1-5). Although individual blinking events produced fewer photons due to 3-5-fold shorter on-times than AF647, the higher number of blinking cycles yielded more localizations and improved image quality. Reconstructions were continuous and dense, confirming the exceptional photostability of JF635b in buffer-independent sb-dSTORM (Fig. 1d, Supp. Table 1).

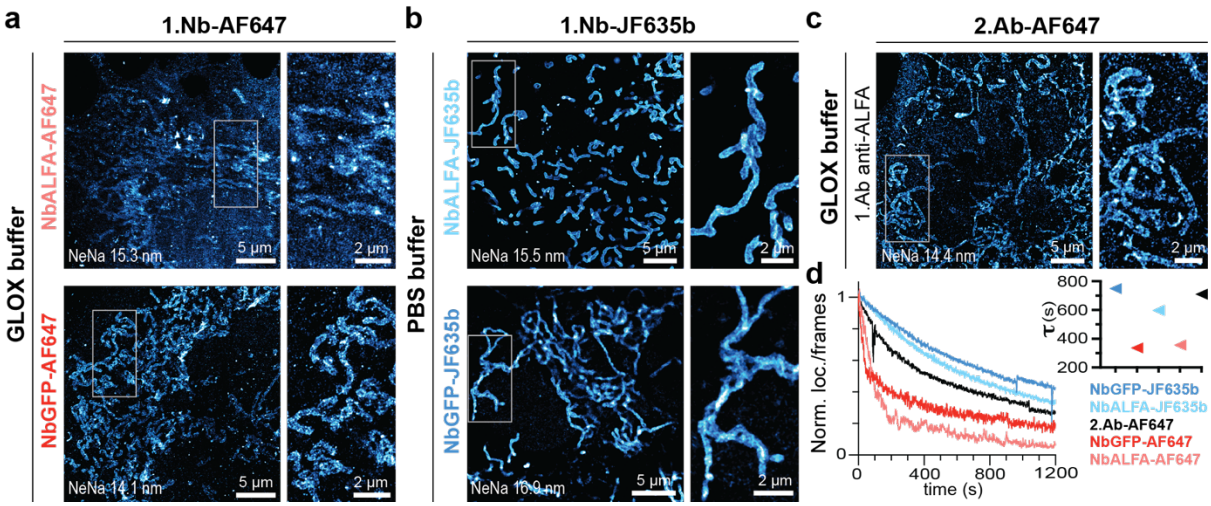

Figure 1. dSTORM using nanobodies conjugated with AF647 and the JF635b. Primary nanobody (1.Nb) NbALFA and NbGFP, each conjugated with 2 AF647 (**a**) or JF635b (**b**), were used to directly label transfected COS-7 cells displaying EGFP and ALFA-tag on their mitochondria. (**c**) As a control, conventional 1.Ab anti-ALFA-tag, revealed by secondary antibodies (2.Ab-AF647). Samples with AF647 were imaged under GLOX-MEA buffer, while samples with JF635b were imaged in PBS. Average localization precisions (NeNa) are indicated above the images. (**d**) Localization per frame was plotted, with the blinking differences between conditions shown as tau (τ) for each curve (details in Methods and Supp. Information).

Although the palette of Nbs expands, the number of direct binders remains limited compared to Abs. Therefore, we turned to secondary nanobodies (2.Nbs), which offer advantages such as easy multiplexing with primary antibodies from the same species and flexibility in using established 1.Abs, while still providing higher localization precision than conventional 2.Abs[15].

We labeled microtubules in COS-7 cells using a monoclonal anti-α-tubulin 1.Ab, revealed with 2.Nbs bearing 2x JF635b per Nb, and imaged them via wide-field sb-dSTORM in PBS (Fig. 2a; Supp. Fig. 2, Supp. Movie 6), and water (Supp. Fig. 3, Supp. Movie 8), expanding its unique feature to be used for Expansion Microscopy (ExM)[16]. Images display continuous microtubule filaments with a localization precision of 12.8±4.5 nm (Fig. 2a) and, using a segmentation tool (Supp. Figure 4), a mesh mean area of 0.77±8.89 µm² was determined (Fig. 2b). Vimentin filaments labeled with a polyclonal rabbit 1.Ab and 2.Nb-JF635b (Fig. 2c; Supp. Fig. 5, Supp. Movie 7) had a similar localization precision of 15.2±4.7 nm and, as expected, a denser mesh with a mean area of 0.15±0.60 µm² (Fig. 2d). Both exhibited high labeling efficiency (additional examples of peroxisome labeling are in Supp. Fig. 6), enabling reliable segmentation and continuous filament visualization. Note that JF635b blinking was consistent across a range of excitation powers, including as low as 5 mW. Optimal results were obtained at 15-20 mW, with an excellent signal-to-noise ratio across 50,000 frames per movie. Remarkably, stained COS-7 samples stored in PBS at 4°C for up to 1 year exhibited

minimal loss of image quality (Supp. Fig. 7). In contrast, AF647 in GLOX-MEA lost blinking within days, and quality declined quickly. Nb-JF635b's stability suggests potential for long-term sample preservation, re-imaging, and high-throughput studies.

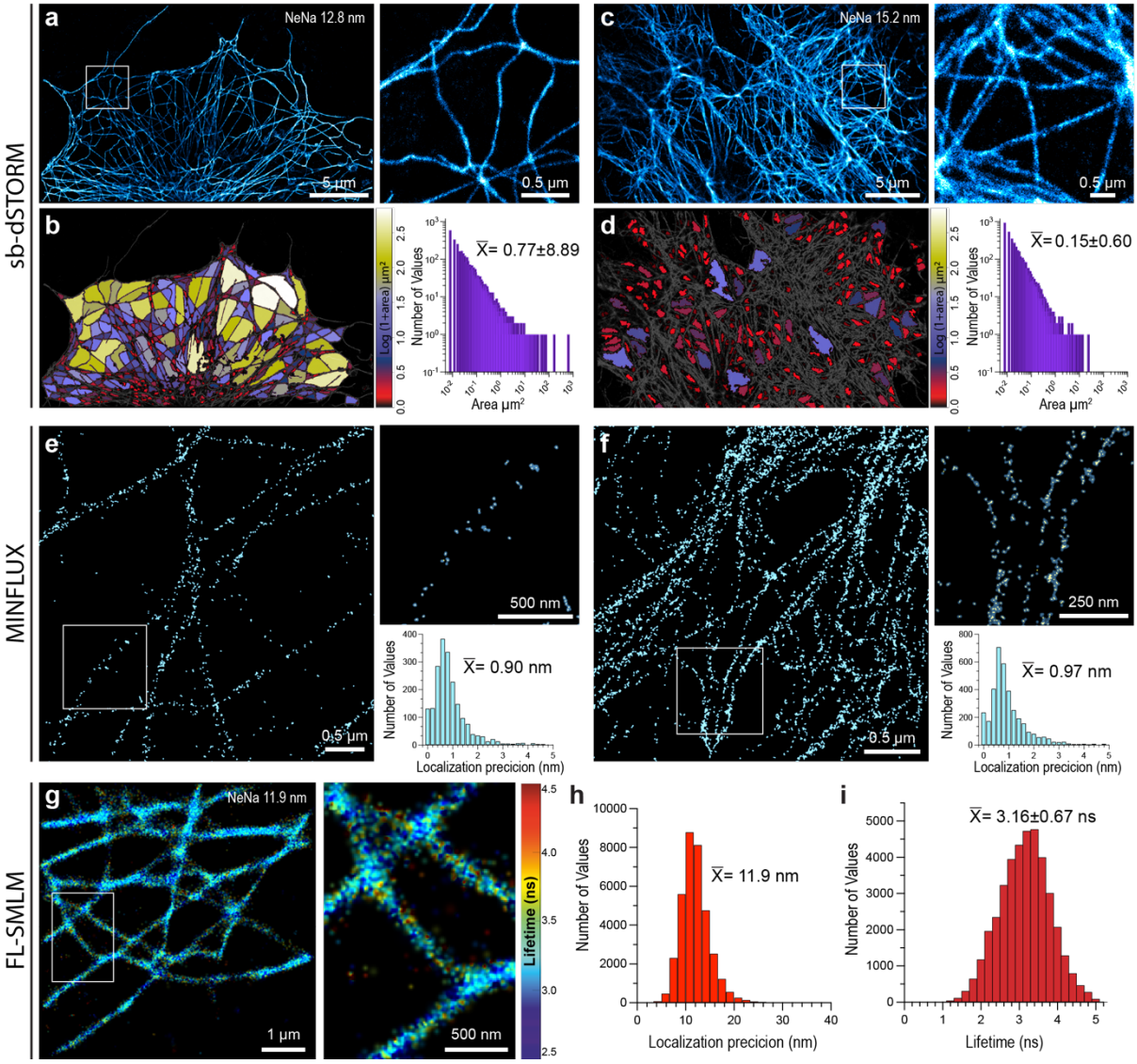

Figure 2. Applications of sb-dSTORM across labeling strategies and SMLM modalities. (**a-d**) Wide-field sb-dSTORM in COS-7 cells labeled with 1.Ab and 2.Nb-JF635b. (**a, c**) Full reconstruction with zoom-ins of microtubule and vimentin. (**b, d**) Segmentation analysis for (a, c) and area histograms for all dataset combined (microtubule, vimentin, respectively). (**e,f**) MINFLUX imaging of the microtubule and vimentin staining using the same labeling strategy as in (a,c). Combined localization precision plots indicate mean precisions of 0.90 nm (microtubules) and 0.97 nm (vimentin). (g-i) Confocal fluorescence lifetime SMLM (FL-SMLM) of microtubules labeled with 1.Ab and 2.Nb-JF635b: (g) Reconstruction, (h) Localization precision histogram, and (i) Fluorescence lifetime distribution with Gaussian fit (mean ± s.d. indicated).

We next explored applications of Nb-assisted sb-dSTORM across different SMLM techniques. First, we benchmarked the performance of Nb-JF635b in MINFLUX[17], a method that achieves sub-nanometer precision by extracting maximal information from relatively low photon counts. Using identical samples prepared as for sb-dSTORM, including fiducial gold

nanoparticles for active drift correction, we achieved mean (combined) localization precisions of 0.90±0.70 nm for microtubules and 0.97±0.75 nm for vimentin (Fig. 2e, f; Supp. Table 2).

Finally, to show the versatility of JF635b when combined with nanobodies, we also tested them using fluorescence-lifetime SMLM (FL-SMLM)[11]. We acquired confocal FL-SMLM datasets (Supp. Fig. 8) of microtubules, and JF635b coupled to Nbs provided a mean localization precision of 11.9±2.9 nm (Fig. 2g-i) and a fluorescence lifetime of 3.16±0.67 ns.

Together, these results show that nanobodies can be used far more reliably in SMLM when conjugated to a self-blinking fluorophore JF635b, which restores robust blinking to Nb conjugates, enables nanometer-scale precision under buffer-independent conditions, and preserves samples for at least 12 months. Its ability to maintain strong blinking even in water underscores the probe's robustness, enhances reproducibility across preparations, and may enable SMLM in techniques such as Expansion Microscopy.

Methods

Cell culture

COS-7 cells were cultured in Petri dishes at 37 °C with 5% CO2 inside a humidified incubator. They were grown in complete Dulbecco's Modified Eagle Medium (DMEM, ThermoFisher Scientific), supplemented with 10% fetal bovine serum (FBS, ThermoFisher), 4 mM L-glutamine, and 1% penicillin/streptomycin (ThermoFisher). For sample preparation, cells were seeded onto 18 mm poly-L-lysine-coated coverslips in 12-well plates and incubated at 37 °C with 5% CO2 in a humidified environment. For transfection, a plasmid encoding TOM70-EGFP-ALFA-tag driven by a CMV promoter was mixed with Lipofectamine 2000 (Thermo Fisher) and added to the seeded cells according to the manufacturer's instructions. Transfection and expression were typically left for 16-18h, before cell fixation.

Immunostaining of cells

COS-7 cells were first treated for 30 s with pre-warmed Extraction Buffer (EB, 10 mM MES, 138 mM KCl,3 mM $MgCl_2$, 2 mM EGTA, 320 mM sucrose, pH 6.8) supplemented with 0.1% Saponin. This was directly followed by fixation in a pre-warmed solution of 4% paraformaldehyde and 0.1% Glutaraldehyde in EB at RT for 15 min. After removing the fixatives and rinsing with PBS, unreacted aldehyde groups were quenched using 100 mM glycine in PBS for 15 min. Cells were blocked and permeabilized with 3% serum albumin

(BSA) and 0.1% Triton X-100 (Sigma-Aldrich) in PBS for 30 min at RT. For Fig. 1, NbGFP and NbALFA labeled with AF647 or JF635b were purchased as FluoTag®-X2 from NanoTag Biotechnologies (clone 1H1, Cat#: N0304; Cat#: N1502) and used at a 1:1000 dilution for 45 minutes. Recombinant anti-ALFA antibody carrying a mouse IgG1 Fc domain (NanoTag Biotechnologies, Cat# N1582) was used at a 1:500 dilution and detected by Goat anti-Mouse IgG (H+L) Cross-Adsorbed Secondary Antibody, Alexa Fluor™ 647, also used in a 1:500 dilution (ThermoFisher, Cat# A-21235). Microtubules and vimentin structures were labeled using a one-step immunofluorescence[15] with a mouse monoclonal (SySy, Cat# 302211) and a rabbit monoclonal (Abcam, Cat# ab92547), respectively. Secondary detection was performed using FluoTag®-X2 anti-Mouse IgG1 (Cat# N2002) or FluoTag®-X2 anti-Rabbit IgG (Cat# N2402). See Supp. Table 3 for details on the used Abs and Nbs. All samples, after staining and washing, were post-fixed in 4% PFA for 15-20 minutes at room temperature, the fixative was removed, and the samples were quenched again with 100 mM glycine in PBS.

Wide-field sb-dSTORM imaging and data analysis

Wide-field sb-dSTORM measurements were performed on a custom-built setup as described previously[4] and in the Supplementary Information. Regions of interest (ROIs) of up to 50 × 50 µm² were recorded with a pixel size in the object plane of 103.5 nm, an exposure time of 30 ms, and an EMCCD gain of 500. Each dataset consisted of 50,000 frames. The laboratory temperature was maintained at 23.0°C to ensure thermal stability of the setup. Linear sample drifts of typically 1-2 pixels were observed during acquisition and were corrected by a cross-correlation algorithm. Excitation was performed using a highly inclined and laminated optical sheet (HILO) configuration with a laser power of ~20 mW, yielding an optimal signal-to-noise ratio. Data analysis has been performed using free software FiJi[18], plugin ThunderSTORM[19]. Same analysis parameters were applied as in previous work[4]. Photostability was quantified by tracking the number of localizations per frame over time (Fig. 1f). Localization tables were exported from the ThunderSTORM plugin as .csv files and processed with a custom Python script to generate photostability plots (cumulative localizations in time, see Fig. 1d). The Photostability curves in Fig. 1d were fitted with an exponential decay, from which characteristic photobleaching times were extracted. Segmentation of reconstructed super-resolution images was carried out using a standard Python image pipeline. Images were preprocessed using intensity filtering and morphological operations to ensure filament continuity and remove non-filament objects, and then inverted to enable analysis of voids rather than filaments. Void regions were then identified (and scaled to 10.35 nm/pixel), border-

adjacent partial objects were removed, and regions were hole-filled to avoid biasing the measurement of their spacing area. Quantitative parameters, including void area distributions, were extracted (see Supplementary Methods for details).

Confocal FL-SMLM sb-dSTORM imaging and data analysis

CLSM measurements were performed using a custom-built confocal microscope as described elsewhere[11,20] and in the Supplementary Information. Regions of interest (ROIs) of 7 × 7 µm² were scanned, each subdivided into 70 × 70 virtual pixels (100nm/pixel). Similar image acquisition parameters were used as in the original FL-SMLM work[11]. During analysis, temporal binning of four consecutive frames was applied to improve signal-to-noise ratio. Data analysis has been performed using custom Matlab-based software TrackNTrace LifetimeEdition[11],freely available at https://github.com/scstein/TrackNTrace/releases/tag/v2.0.

MINFLUX sb-dSTORM imaging

MINFLUX sb-dSTORM measurements were performed on a commercial MINFLUX nanoscope (Abberior Instruments GmbH, Göttingen) controlled by *Imspector* software. Data were acquired using the standard 2D acquisition protocol described by Sahl *et al.*[21]. Gold colloid particles (150 nm; BBI Solutions, catalogue no. EM.GC150/4, Crumlin, UK) were added to the samples as fiducial markers for active beam-path drift correction.

Regions of interest (ROIs) of 5 × 5 µm² were acquired over a total measurement time of ~6 h. Excitation was performed with the 642 nm laser at 5-10% output (~25-50 µW) as part of the MINFLUX localization routine. Image data were saved as MSR files and processed in MATLAB (MathWorks, USA).

Localization precisions were calculated as described previously[22]. In brief, localizations from binding events with more than four detections were combined. For enhanced visualization, MINFLUX images were rendered in Blender 3.4.1: raw localizations were displayed as overlapping blue spheres (20 nm) to illustrate the spread of individual events, while combined localizations were rendered as gold spheres (10 nm) to indicate the most likely fluorophore positions.

Data Availability

All data supporting the conclusions of this study are available from the corresponding authors upon reasonable request.

Code availability

FiJi: https://fiji.sc/

Fiji ThunderSTORM plugin: https://github.com/zitmen/thunderstorm

TrackNTrace https://github.com/NRadmacher/TrackNTrace/tree/ISM;

Abberior Imspector commercially available from Abberior Instruments GmbH, Göttingen, Germany

Funding

S.B. is grateful to the European Research Council (ERC) through the project "smMIET" (Grant agreement No. 884488) under the European Union's Horizon 2020 research and innovation program. F.O. acknowledges the support by Deutsche Forschungsgemeinschaft (DFG) through the SFB1286 (project Z04). Y.G.P. acknowledges support from the DFG, Project-ID 449750155, RTG 2756. S.J. acknowledges support from the DFG (FOR2848, P04).

Acknowledgements

The authors are grateful to Jannik Hentze for their help with sample preparation and labeling. The authors thank Dr. Peter Ilgen (Fraunhofer ITMP, Göttingen) for MINFLUX data visualization using Blender. The authors are grateful to Dr. Antonio Politi (MPI-NAT, Göttingen) for advice in developing the segmentation analysis pipeline. The authors are thankful to Dr. Steffen Frey (NanoTag GmbH) for advice. We thank Prof. Philip Tinnefeld's lab (LMU, Munich) for support with JF635b blinking experiments in water. The authors are grateful to Ingo Gregor for technical assistance.

Competing interests

F.O. is a shareholder of NanoTag Biotechnologies GmbH. All other authors declare no competing interests.

Additional information

Supplementary information is available for this paper.

References

1. Lelek, M. *et al.* Single-molecule localization microscopy. *Nat Rev Methods Primers* **1**, 1–27 (2021).
2. Dempsey, G. T., Vaughan, J. C., Chen, K. H., Bates, M. & Zhuang, X. Evaluation of fluorophores for optimal performance in localization-based super-resolution imaging. *Nat Methods* **8**, 1027–1036 (2011).
3. Mougios, N. *et al.* NanoPlex: a universal strategy for fluorescence microscopy multiplexing using nanobodies with erasable signals. *Nat Commun* **15**, 8771 (2024).
4. Sograte-Idrissi, S. *et al.* Nanobody Detection of Standard Fluorescent Proteins Enables Multi-Target DNA-PAINT with High Resolution and Minimal Displacement Errors. *Cells* **8**, 48 (2019).
5. Uno, S. *et al.* A spontaneously blinking fluorophore based on intramolecular spirocyclization for live-cell super-resolution imaging. *Nature Chem* **6**, 681–689 (2014).
6. Yang, Q. *et al.* Self-Blinking Thioflavin T for Super-resolution Imaging. *J. Phys. Chem. Lett.* **15**, 7591–7596 (2024).
7. Jradi, F. M. *et al.* Coumarin as a general switching auxiliary to prepare photochromic and spontaneously blinking fluorophores. *bioRxiv* 2024.05.12.593749 (2024) doi:10.1101/2024.05.12.593749.
8. Remmel, M., Scheiderer, L., Butkevich, A. N., Bossi, M. L. & Hell, S. W. Accelerated MINFLUX Nanoscopy, through Spontaneously Fast-Blinking Fluorophores. *Small* **19**, 2206026 (2023).
9. Grußmayer, K., Lukes, T., Lasser, T. & Radenovic, A. Self-Blinking Dyes Unlock High-Order and Multiplane Super-Resolution Optical Fluctuation Imaging. *ACS Nano* **14**, 9156–9165 (2020).
10. Holland, K. L. *et al.* A series of spontaneously blinking dyes for super-resolution microscopy. 2024.02.23.581625 Preprint at https://doi.org/10.1101/2024.02.23.581625 (2024).
11. Thiele, J. C. *et al.* Confocal Fluorescence-Lifetime Single-Molecule Localization Microscopy. *ACS Nano* **14**, 14190–14200 (2020).
12. Oleksiievets, N. *et al.* Fluorescence lifetime DNA-PAINT for multiplexed super-resolution imaging of cells. *Commun Biol* **5**, 1–8 (2022).
13. Balzarotti, F. *et al.* Nanometer resolution imaging and tracking of fluorescent molecules with minimal photon fluxes. *Science* **355**, 606–612 (2017).
14. Götzke, H. *et al.* The ALFA-tag is a highly versatile tool for nanobody-based bioscience applications. *Nat Commun* **10**, 4403 (2019).
15. Sograte-Idrissi, S. *et al.* Circumvention of common labelling artefacts using secondary nanobodies. *Nanoscale* **12**, 10226–10239 (2020).
16. Chen, F., Tillberg, P. W. & Boyden, E. S. Expansion microscopy. *Science* **347**, 543–548 (2015).
17. Masullo, L. A. *et al.* Pulsed Interleaved MINFLUX. *Nano Lett.* **21**, 840–846 (2021).
18. Schindelin, J. *et al.* Fiji: an open-source platform for biological-image analysis. *Nat Methods* **9**, 676–682 (2012).

19. Ovesný, M., Křížek, P., Borkovec, J., Švindrych, Z. & Hagen, G. M. ThunderSTORM: a comprehensive ImageJ plug-in for PALM and STORM data analysis and super-resolution imaging. *Bioinformatics* **30**, 2389–2390 (2014).
20. Oleksiievets, N. *et al.* Single-Molecule Fluorescence Lifetime Imaging Using Wide-Field and Confocal-Laser Scanning Microscopy: A Comparative Analysis. *Nano Lett.* **22**, 6454–6461 (2022).
21. Sahl, S. J. *et al.* Direct optical measurement of intramolecular distances with angstrom precision. *Science* **386**, 180–187 (2024).
22. Ostersehlt, L. M. *et al.* DNA-PAINT MINFLUX nanoscopy. *Nat Methods* 1–4 (2022) doi:10.1038/s41592-022-01577-1.